Supporting Information

Zeolite CAN and AFI-Type Zeolitic Imidazolate Frameworks with Large 12-Membered Ring Pore Openings Synthesized Using Bulky Amides as Structure-Directing Agents

Qi Shi,[a] Wei-Jian Xu,[b] Rui-Kang Huang,[b] Wei-Xiong Zhang,*,[b] Yang Li,[b] Pengfei Wang,[c] Fa-Nian Shi,*,[d] Libo Li[a], Jinping Li,[a] and Jinxiang Dong*,[a]

[a] College of Chemistry and Chemical Engineering, Taiyuan University of Technology, Taiyuan, 030024, China, E-mail: dongjinxiangwork@hotmail.com

[b] MOE Key Laboratory of Bioinorganic and Synthetic Chemistry, School of Chemistry, Sun Yat-Sen University, Guangzhou, 510275, China, E-mail: zhangwx6@mail.sysu.edu.cn

[c] Analytical Instrumentation Center, Institute of Coal Chemistry, Chinese Academy of Sciences, Taiyuan, 030001, China

[d] School of Science, Shenyang University of Technology, Shenyang, 110870, China, E-mail: fshi96@foxmail.com

Table of Contents

Section S1. Materials and Instrumentation

Materials: Imidazole (Im, 99.0 %), zinc acetate dihydrate ($Zn(OAc)_2 \cdot 2H_2O$, 98.0 %) were purchased from Sigma-Aldrich Chemical Co., *N*,*N*-dipropylformamide (DPF, 96.0 %) were obtained from Meryer (Shanghai) Chemical Technology Co., Ltd., and *N*,*N*-dibutylformamide (DBF, 98.0 %) were obtained from TCI (Shanghai) Development Co. Ltd.. All raw chemicals were used without further purification.

Instrumentation: PXRD patterns were recorded with a X-ray diffractometer (Rigaku, MiniFlex Ⅱ) using $Cu_{K\alpha}$ radiation (λ=1.5418 Å). TG measurements were performed under a static air atmosphere on a simultaneous thermal analyzer (Setaram, Labsys evo) at a heating rate of 5 °C min^{-1}. CHNO analysis was carried out on an elemental analyzer (Elementar, Vario EL III). The contents of Zn were determined by inductively coupled plasma-atomic emission spectrometry (Leeman, Profile-Spec). Nitrogen sorption isotherms were measured by using an automated volumetric adsorption apparatus (Micromeritics, ASAP2020). $^{1}H \rightarrow {}^{13}C$ cross-polarization (CP) magic angle spinning (MAS) NMR spectroscopy was performed on a Bruker Avance III 600 WB spectrometer at 151 MHz at a magnetic field of 14.2 T using a 4 mm double-tuned MAS probe with a spinning speed of 10.5 kHz. SEM micrographs were obtained with a scanning electron microscope (Hitachi, TM3000). TEM images were recorded on a Transmission electron microscope (JEOL, JEM-2010).

Section S2. Single-crystal X-ray crystallography for CAN-[Zn(Im)$_2$] and the Rietveld analysis of AFI-[Zn(Im)$_2$].

Single-crystal X-ray crystallography for CAN-[Zn(Im)$_2$].

Single crystal X-ray diffraction data collection for the CAN-[Zn(Im)$_2$] was performed on an Agilent Xcalibur Eos Gemini CCD plate diffractometer operating using graphite monochromatized $Cu_{K\alpha}$ radiation (λ = 1.54184 Å) at 293 K. CRYSALIS CCD and RED software were used for data collection and processing, respectively. The reflection intensities were corrected for absorption using the multi-scan method. The structures were solved by direct methods using SHELXS-97[1] and refined on F^2 by the full matrix least-squares method using SHELXL-97.[2] All the non-hydrogen atoms were refined anisotropically. The solvent molecules (DBF) in the 12-membered ring were severely disordered and were refined using the PART command. All H atoms were refined isotropically. The final full matrix least-squares refinement on F^2 converged to R_1 = 0.1144 (I > 2sigma (I)) and wR_2 = 0.3168 (all data) with GOF = 1.058. For the structure without the guest molecules (CAN-[Zn(Im)$_2$]) by using the SQUEEZE option, the final full matrix least-squares refinement on F^2 converged to R_1 = 0.0833 (I > 2sigma (I)) and wR_2= 0.1756 (all data) with GOF = 1.047. The detailed crystallographic data and structural refinement parameters are summarized in Table S4 (CAN-[Zn(Im)$_2$]) and S5 (CAN-[Zn(Im)$_2$], without the guest molecules). CCDC 1509275 (CAN-[Zn(Im)$_2$]) and 1509089 (CAN-[Zn(Im)$_2$], without the guest molecules) contain the supplementary crystallographic data for this paper. These data are provided free of charge by The Cambridge Crystallographic Data Centre.

References

1. Sheldrick, G. M. SHELXS-97, Program for Crystal Structure Solution, University of Göttingen, Germany, 1997.
2. Sheldrick, G. M. SHELXL-97, Program for Crystal Structure Refinement, University of Göttingen, Germany, 1997.

The Rietveld analysis of AFI-[Zn(Im)$_2$] (without the guest molecules).

a) Data collection: The X-ray powder diffraction data for structure refinement was collected on a Bruker D8 Advance using $Cu_{K\alpha}$ X-ray radiation (40 kV, 40 mA). The step-scanned X-ray powder diffraction data was recorded in the 2θ range of 3–69° with a 2θ step of 0.02° and scan speed of 5 seconds/step.

b) Structural model and Rietveld refinement: The indexing and refinement of the PXRD patterns were carried out using the Reflex module of Material Studio 5.0. The pattern was well indexed in a hexagonal primitive cell: a = 26.374 Å, c = 16.739 Å. The Pawley refinement was then performed in the 2θ range of 3-69° on the unit-cell parameters, zero point, background terms with Pseudo–Voigt profile function and Berar–Baldinozzi asymmetry correction function, and yielded the hexagonal cell with the unit cell parameters: a = 24.468 Å, c = 16.621 Å, R_p = 3.60 % and R_{wp} = 5.54 %. Considering the cell was close to the cell of a hypothetical ZIF with a structure model celled AFI (a = 26.875 Å, b = 26.915 Å, c =

16.574 Å, α = 90.02°, β = 89.99°, γ = 119.88°) reported in the literature[1], a reasonable structure model in the space group *P*6/*mcc* was constructed as an initial structure model for the Rietveld refinement. The final refinement resulted in the following cell parameters and *R*-factors: *a* = 26.437 Å, *c* = 16.632 Å, R_p = 5.73 % and R_{wp} = 9.18 %. The results of the Rietveld analysis of the structure without the guest molecules have been summarized in Table S6 (AFI-[Zn(Im)$_2$]). CCDC 1509111 (AFI-[Zn(Im)$_2$]) contain the supplementary crystallographic data for this paper. These data are provided free of charge by The Cambridge Crystallographic Data Centre.

References

1. Lewis, D. W.; Ruiz-Salvador, A. R.; Gómez, A.; Rodriguez-Albelo, L. M.; Coudert, F. X.; Slater, B.; Cheetham, A. K.; Mellot-Draznieks, C. *CrystEngComm* **2009**, *11*, 2272–2276.

Section S3. Synthesis of CAN-[$Zn(Im)_2$] and AFI-[$Zn(Im)_2$].

Synthesis of CAN-[$Zn(Im)_2$].

A solution Im (2.0 mmol, 0.136 g) in DBF (4 mL) was added to a solution of $Zn(OAc)_2$•$2H_2O$ (0.4 mmol 0.088 g) in DBF (4 mL) in a 20 mL Teflon-lined stainless-steel autoclave. The autoclave was heated at 40 ^oC for 3 d and then cooled to room temperature. A pure phase of white rod-shaped crystals were collected by filtration, washed three times using acetone and dried under ambient conditions (Yield: 0.09 g). Prior to the N_2 sorption measurement, the as-synthesized sample was immersed in dry acetone for 48 h. Then, the sample was separated by centrifugation and dried at ambient temperature. Before the measurement, the samples were activated again using the "degas" function of the surface area analyzer for 2 h at 50 °C.

Elemental analysis (%) for $C_{31.5}H_{46.5}N_{13.5}O_{1.5}Zn_3$ = $Zn_3(Im)_6$·1.5DBF : calcd: C 45.34, H 5.62, N 22.67, O 2.88, Zn 23.50 ; found: C 46.41, H 5.77, N 22.29, O 3.00, Zn 23.54.

Elemental analysis (activated, %) for $C_{18}H_{18}N_{12}Zn_3$ = $Zn_3(Im)_6$: calcd: C 36.12, H 3.01, N 28.10, Zn 32.76 ; found: C 36.86, H 3.12, N 27.71, Zn 33.12.

Synthesis of AFI-[$Zn(Im)_2$].

A solution of $Zn(OAc)_2$•$2H_2O$ (1.0 mmol, 0.220 g) in DPF (5 mL) was a solution Im (4.0 mmol, 0.272 g) in DPF (10 mL) added to in a 20 mL Teflon-lined stainless-steel autoclave. The autoclave was heated at 60 ^oC for 3 d and then cooled to room temperature. A pure phase of powers were collected by filtration, washed three times using acetone and dried under ambient conditions (Yield: 0.21 g). Prior to the N_2 sorption measurement, the as-synthesized sample was immersed in dry acetone for 48 h. Then the sample was separated by centrifugation and dried at ambient temperature. Before the measurement, the samples were activated again by using the "degas" function of the surface area analyzer for 2 h at 50 °C.

Elemental analysis (%) for $C_{11.6}H_{18}N_{4.8}O_{0.8}Zn$= $Zn(Im)_2$·0.8 DPF: calcd: C 45.99, H 6.00, N 22.20, O 4.23, Zn 22.20 ; found: C 45.76, H 5.82, N 21.95, O 4.10, Zn 22.77.

Elemental analysis (activated, %) for $C_6H_6N_4Zn$= $Zn(Im)_2$: calcd: C 36.12, H 3.01, N 28.10, Zn 32.76 ; found: C 36.70, H 3.20, N 27.32, Zn 31.47.

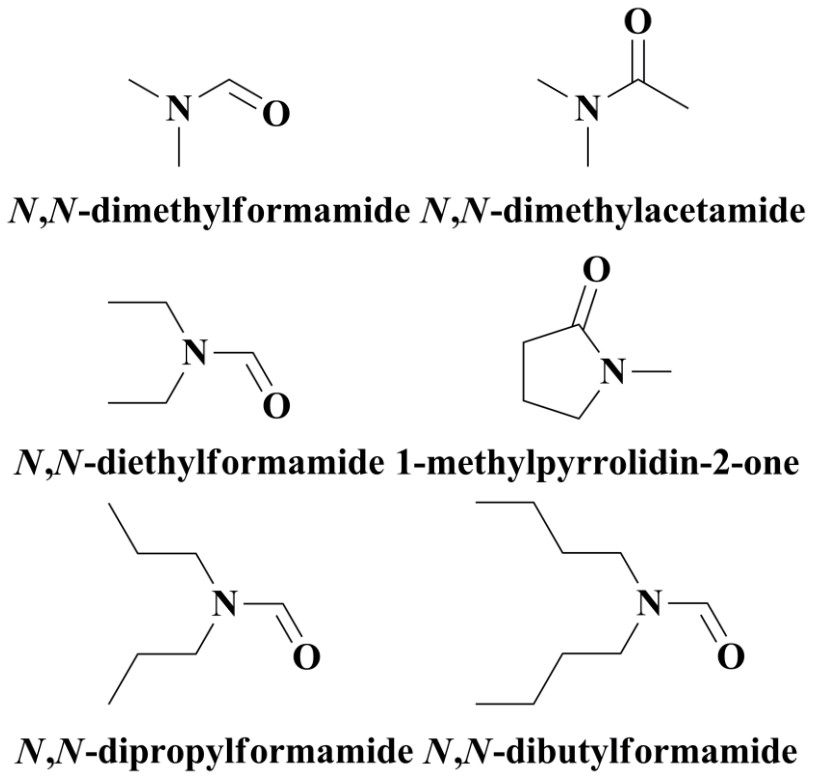

Scheme S1 The structural formula of N,N-dimethylformamide (DMF), N,N-dimethylacetamide (DMA), N,N-diethylformamide (DEF), N-methylpyrrolidone/1-Methylpyrrolidin-2-one (NMP), N,N-dipropylformamide (DPF), and N,N-dibutylformamide (DBF).

The ZIFs have been typically synthesized using small amide solvent, such as DMF, DMA, DEF and NMP. In this article, bulky and commercially available amide DBF and DPF were used for ZIFs synthesis.

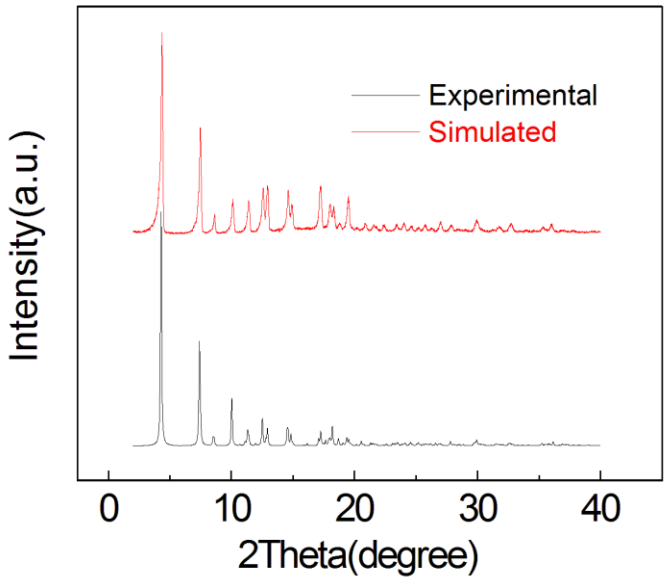

Figure S1. Experimental XRD pattern of sample CAN-[Zn(Im)$_2$] and XRD pattern simulated from crystal structure data.

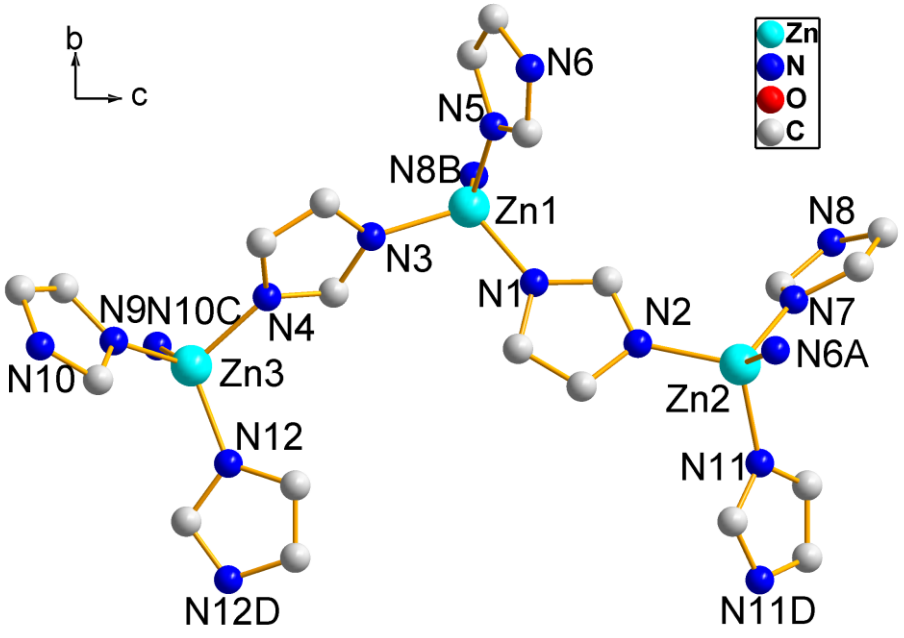

Figure S2. Coordination environment around Zn centers within the asymmetric unit of CAN-[Zn(Im)$_2$]. Hydrogen atoms and guests were omitted for clarity. Symmetry Operation: A, 1-x, 1-y, 2-z; B, 2-x, 1-y, 2-z; C, 0.5+x , y, 1.5-z; D, x, 0.5-y, z.

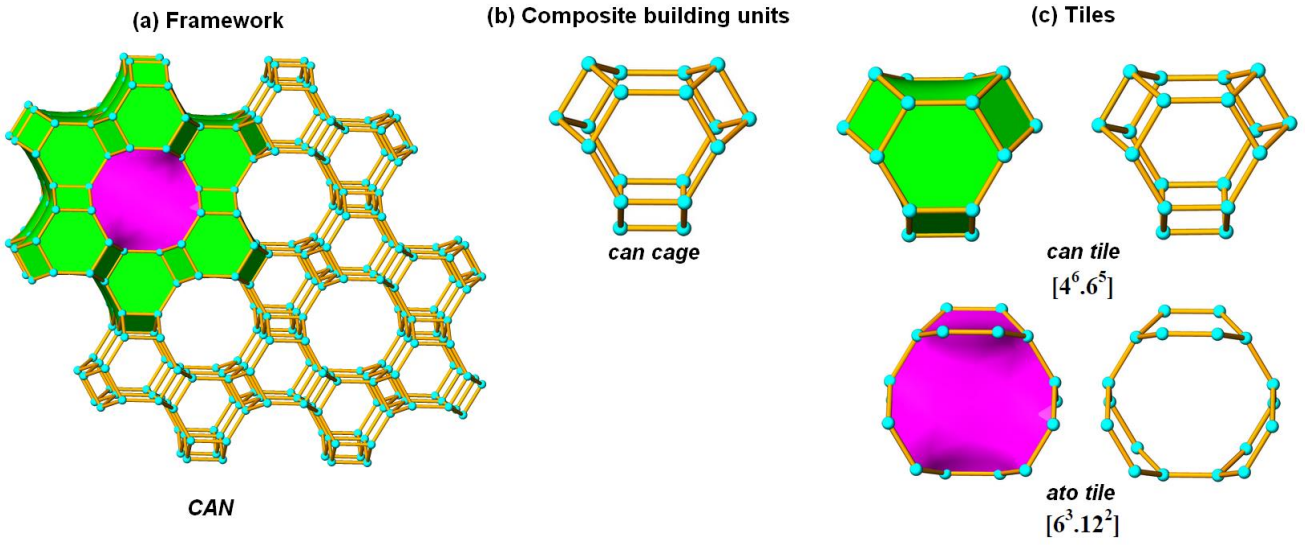

Figure S3. Composite building units (b) and tiles (c) in the framework CAN-[$Zn(Im)_2$] (a).

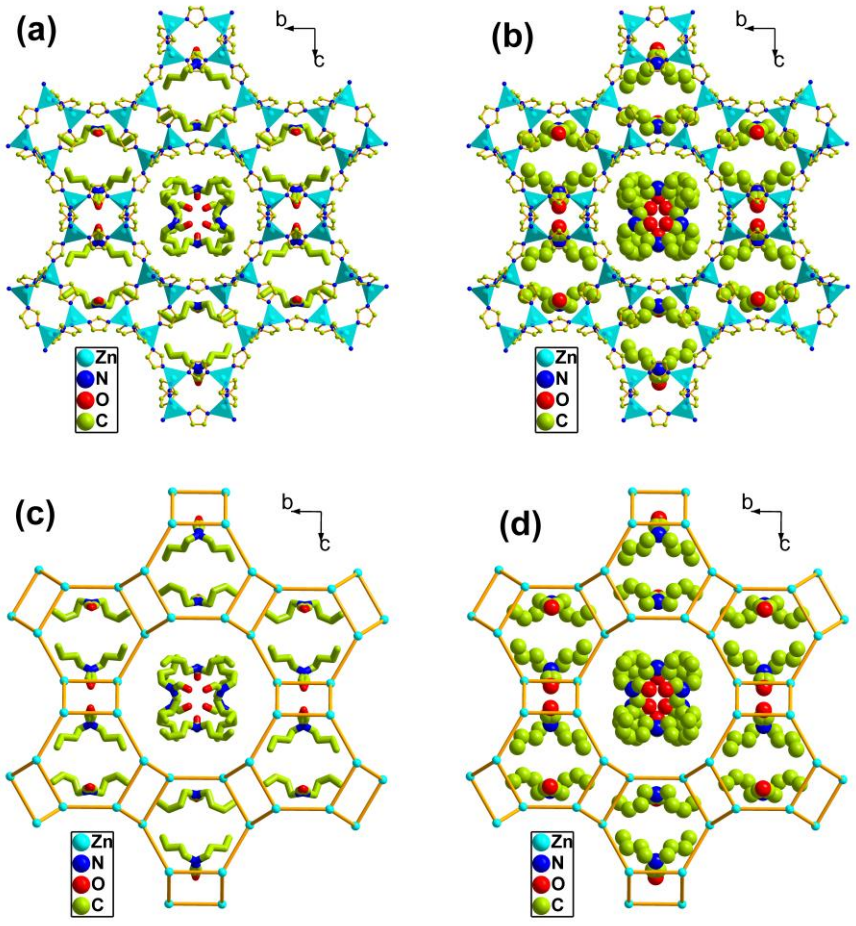

Figure S4. The distribution of DBF in the framework of CAN-[$Zn(Im)_2$]: (a) stick models, and (b) space filling; the distribution of DBF in the topological structure of CAN-[$Zn(Im)_2$]: (c) stick models, and (d) space filling

There were two different disordered DBF guestsinthe channels of the 12-MR, one DBF molecule was disordered over two positions and another DBF molecule was disordered over four positions.

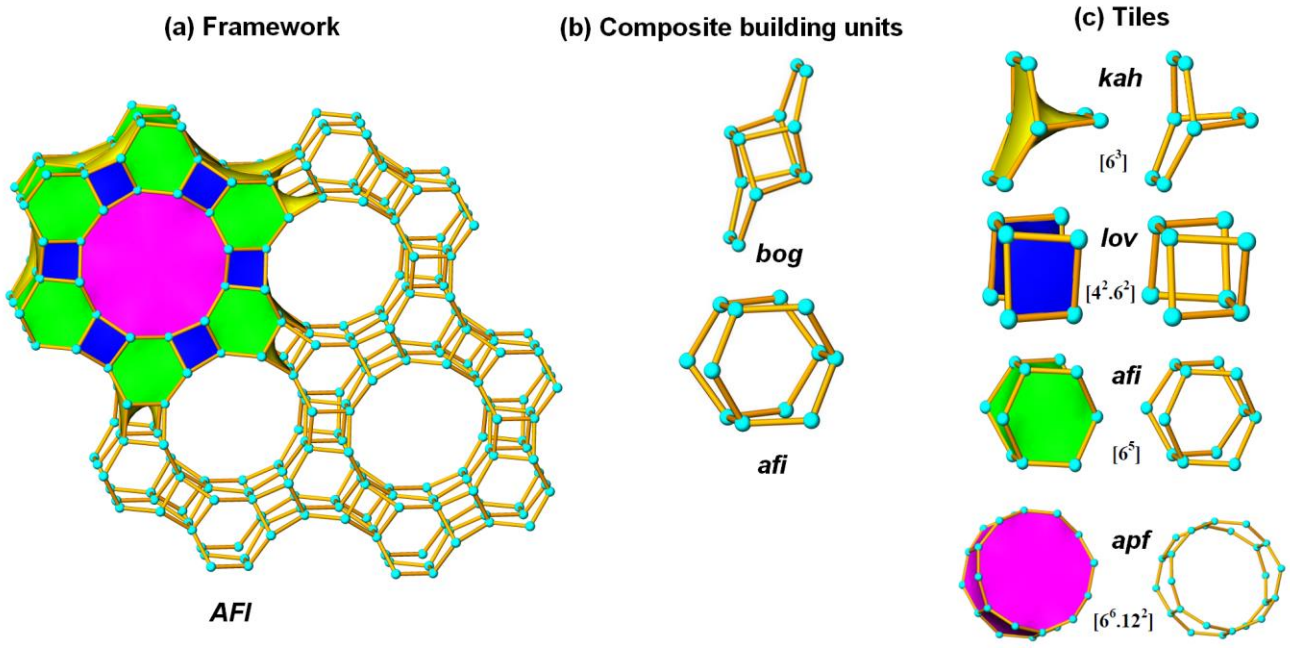

Figure S5. Composite building units (b) and tiles (c) in the framework AFI-[$Zn(Im)_2$] (a).

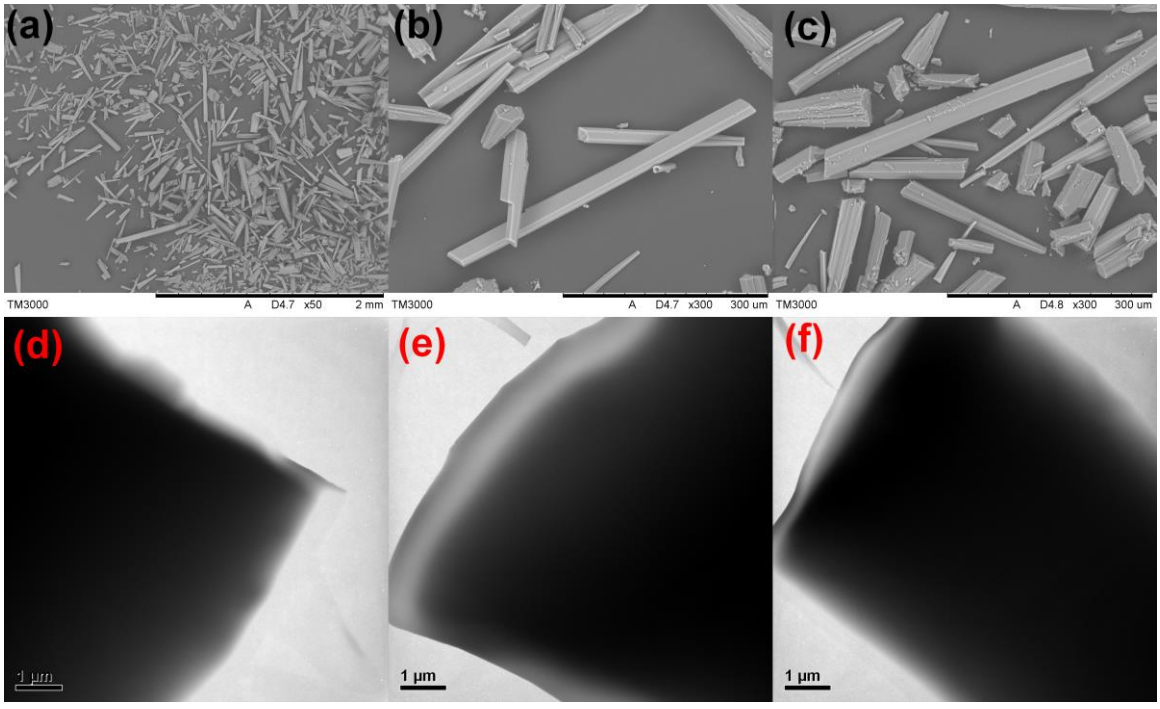

Figure S6 (a, b, c) Different magnification SEM images of as-synthesized CAN-[$Zn(Im)_2$] samples and (d, e, f) TEM images taken from terminal region of some individual crystals of CAN-[$Zn(Im)_2$].

The morphology of as-synthesized CAN-[$Zn(Im)_2$] samples was examined by SEM and TEM as shown in Figure S6. The low-magnification SEM image (Figure S6a) reveals that the product consisted of rod-shaped crystal. Based on high-magnification SEM images (Figure S6b and S6c), the typical individual crystals of CAN-[$Zn(Im)_2$] have a size in the range of 400–500 µm. Figure S6d, S6e, and S6f are TEM images taken from terminal region of some individual crystals.

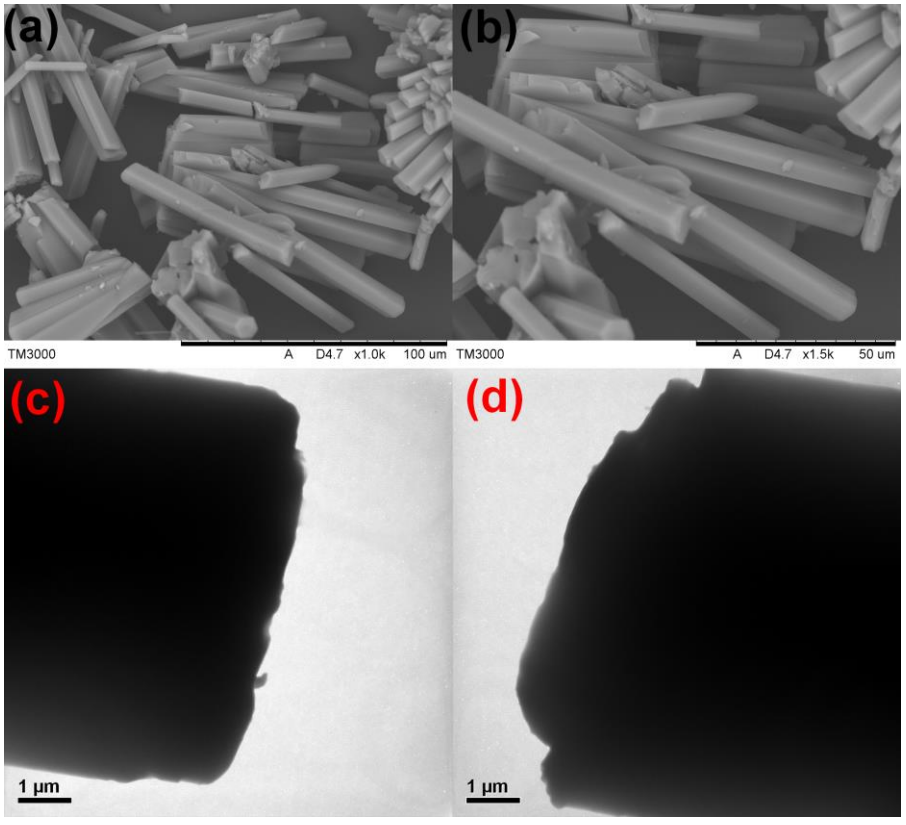

Figure S7 (a, b) Different magnification SEM images of as-synthesized AFI-[$Zn(Im)_2$] samples and (c, d) TEM images taken from terminal region of some individual crystals of AFI-[$Zn(Im)_2$].

The morphology of as-synthesized AFI-[$Zn(Im)_2$] samples was examined by SEM and TEM as shown in Figure S7. Based on SEM results (Figure S7a and S7b), as-synthesized AFI-[$Zn(Im)_2$] samples show the rod morphology with a size of about 50-100 µm. Figure S6c, and S6d are TEM images taken from terminal region of some individual crystals.

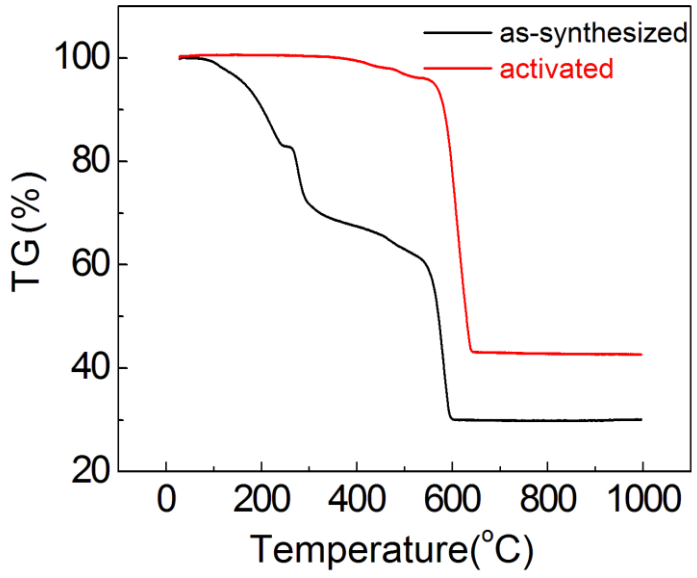

Figure S8. The TG curves of as-synthesized and activated CAN-[$Zn(Im)_2$] samples.

It is noticeable that the mass loss of sample CAN-[$Zn(Im)_2$] from RT to 300 ^oC is about 28.2 wt%, which closely matches DBF molecule calculated from the formula $Zn_3(Im)_6$•1.5DBF (28.3 wt.%) . The solid residue (30.0 wt.%) obtained after TG was ZnO (calculated: 29.2 wt.%).

In TG analysis of activated sample CAN-[$Zn(Im)_2$], a long plateau was observed at temperatures up to 300 °C, at which decomposition of the framework structure commenced. The solid residue (42.6 wt.%) obtained after TG was ZnO (calculated from the formula $Zn_3(Im)_6$: 40.8 wt.%). It has been shown that guest molecule DBF in the framework may be removed.

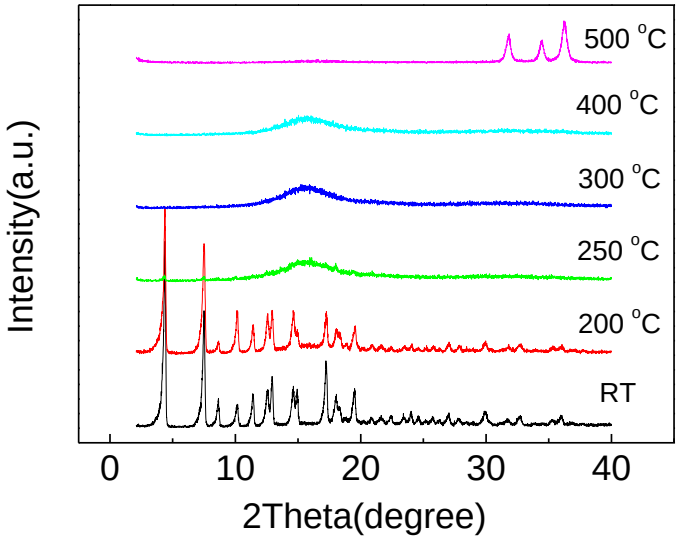

Figure S9. PXRD patterns taken from CAN-[$Zn(Im)_2$] samples that had been heated to different temperatures in air for 5 h.

The PXRD patterns demonstrate that the framework structure of the CAN-[$Zn(Im)_2$] samples remains stable up to at least 200 °C for 5 h. However, the characteristic PXRD peaks of CAN-[$Zn(Im)_2$] start disappearing in the patterns of samples that had been heated to 250 °C for 5 h. Continued heating to above 500 °C resulted in the formation of ZnO.

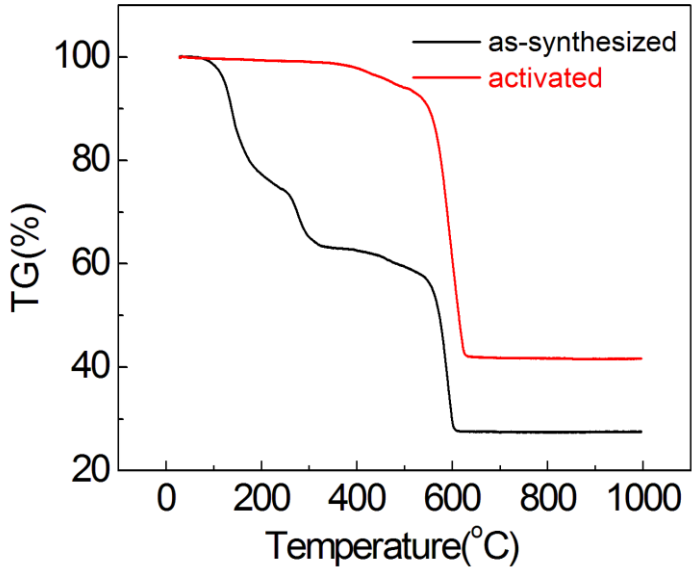

Figure S10. The TG curves of as-synthesized and activated AFI-[$Zn(Im)_2$] samples.

TG analysis of samples AFI-[$Zn(Im)_2$] shows a ca. 34.7 wt.% weight loss from RT to 300 ^{o}C, which was assigned to the loss of 0.8 DPF molecules and is in good agreement with the calculated values (calculated form the formula $Zn(Im)_2 \cdot 0.8$ DPF: 34.2 wt.%). The solid residue (26.5 wt.%) obtained after TG was ZnO (calculated: 26.9 wt.%).

In TG analysis of activated sample AFI-[$Zn(Im)_2$], a long plateau was observed at temperatures up to 300 °C, at which decomposition of the framework structure commenced. The solid residue (41.6 wt.%) obtained after TG was ZnO (calculated from the formula $Zn(Im)_2$: 40.8 wt.%). It has been shown that guest molecule DPF in the framework may be removed.

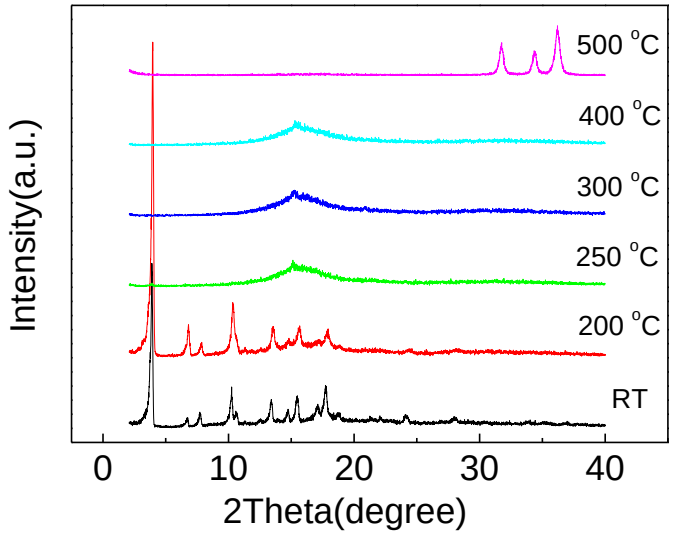

Figure S11. PXRD patterns taken from AFI-[$Zn(Im)_2$] samples that had been heated to different temperatures in air for 5 h.

The PXRD patterns demonstrate that the framework structure of the AFI-[$Zn(Im)_2$] samples remains stable up to at least 200 °C for 5 h. However, the characteristic PXRD peaks of AFI-[$Zn(Im)_2$] start disappearing in the patterns of samples that had been heated to 250 °C for 5 h. Continued heating to above 500 °C resulted in the formation of ZnO.

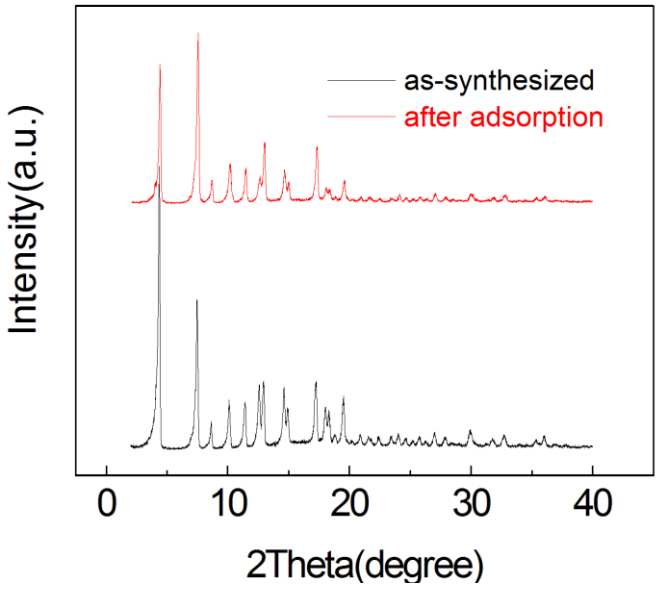

Figure S12. PXRD patterns of CAN-[$Zn(Im)_2$] before adsorption and after adsorption.

The sample after adsorption was characterized by XRD to confirm that it has the same structure with as-synthesized sample.

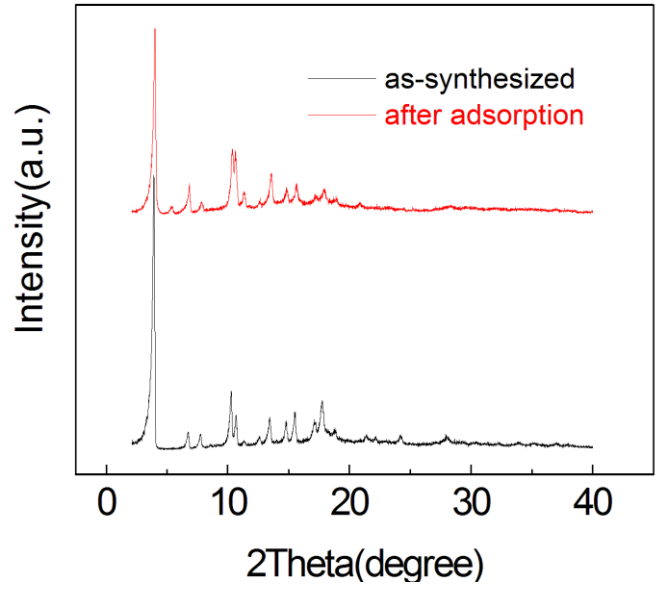

Figure S13. PXRD patterns of AFI-[$Zn(Im)_2$] before adsorption and after adsorption.

The sample after adsorption was characterized by XRD to confirm that it has the same structure with as-synthesized sample.

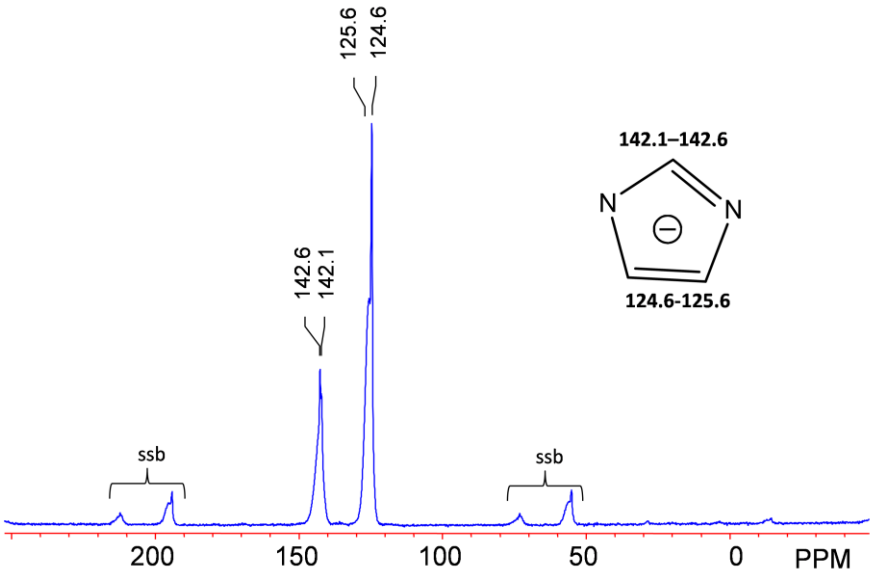

Figure S14. $^{13}C\{^{1}H\}$ MAS solid-state NMR spectra of the activated CAN-[$Zn(Im)_2$] samples (ssb are the spinning side bands).

The absence of peaks corresponding to DBF indicates that the activated samples was fully desolvated under the conditions of the sorption experiment.

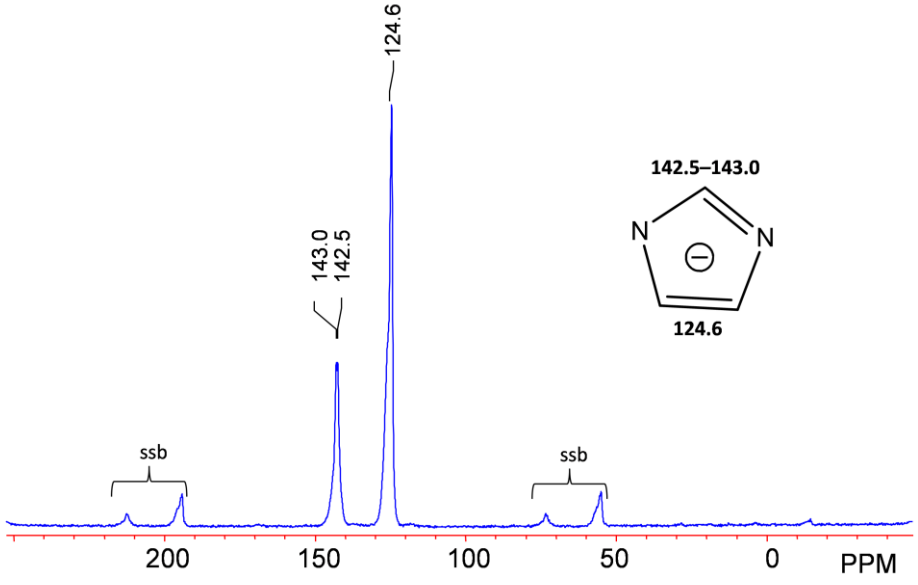

Figure S15. $^{13}C\{^{1}H\}$ MAS solid-state NMR spectra of the activated AFI-$[Zn(Im)_2]$ samples (ssb are the spinning side bands).

The absence of peaks corresponding to DPF indicates that the activated samples was fully desolvated under the conditions of the sorption experiment.

Table S1. Topology, n-MR pore opening, pore aperture diameter, and textural properties of all ZIF topologies contain large 12-MR reported thus far[1]. (MR=membered ring)

RCSR topoIogy or zeolite code	Type material	Framework formula[a]	n-MR pore opening	Pore aperture diameter[b], Å	Surface area (Langmuir) $m^2 g^{-1}$	Surface area (BET) $m^2 g^{-1}$	Pore volume $cm^3 g$	Ref.
GME	ZIF-70	$Zn(Im)_{1.13}(nIm)_{0.87}$	12	13.1	1970	1730	-	2
poz	ZIF-95	$Zn(clbIm)_2$	12	3.7	1240	1050	0.43	3
moz	ZIF-100	$Zn_{20}(clbIm)_{39}(OH)$	12	3.4	780	595	0.37	3
zea	TIF-1	Zn(dmbIm)	16	11.7	667.5	-	0.231	4
zeb	TIF-2	$Zn(Im)_{1.1}(mbIm)_{0.9}$	12	9.6	618.2	-	0.206	5
CAN	**CAN-$[Zn(Im)_2]$**	**$Zn_3(Im)_6$**	**12**	**13.2 (12.7[c])**	**1401**	**1178**	**0.54**	**Our**
AFI	**AFI-$[Zn(Im)_2]$**	**$Zn(Im)_2$**	**12**	**15.6 (18.4[c])**	**1628**	**1386**	**0.64**	**Our**

a: Im=imidazolate; nIm=2-nitroimidazolate; clbIm=5-chlorobenzimidazolate; dmbIm=5,6-dimethylbenzimidazolate; mbIm=5-methylbenzimidazolate.

b: is the diameter of the largest sphere that will pass through the pore.

c: It was calculated by the DFT model using the N_2 isotherm.

(1) Phan, A.; Doonan, C. J.; Uribe-Romo, F. J.; Knobler, C. B.; O'Keeffe, M.; Yaghi, O. M. *Acc. Chem. Res.* **2010**, *43*, 58–67.

(2) Banerjee, R.; Phan, A.; Wang, B.; Knobler, C.; Furukawa, H.; O'Keeffe, M.; Yaghi, O. M. *Science* **2008**, *319*, 939–943.

(3) Wang, B.; Côté, A. P.; Furukawa, H.; O'Keeffe, M.; Yaghi, O. M. *Nature* **2008**, *453*, 207–211.

(4) Wu, T.; Bu, X. H.; Liu, R.; Lin, Z. E.; Zhang, J.; Feng, P. Y. *Chem. Eur. J.* **2008**, *14*, 7771–7773.

(5) Wu, T.; Bu, X. H.; Zhang, J.; Feng, P. Y. Chem. Mater. 2008, 20, 7377–7382.

Table S2. Topology, structure-directing agent, and n-MR pore openings of all $Zn(Im)_2$ polymorphs reported thus far[1](two examples of $Zn_4(Im)_8(HIm)$ and $Zn(Im)_{1.7}(mIm)_{0.3}$ were also added). (Im=imidazolate; HIm=imidazole; mIm=2-methylimidazolate; MR=membered ring)

RCSR topoIogy or zeolite code	Name (CCDC code)	Framework formula	solvent or structure-directing agent[a]	n-MR Pore Opening	Ref.
zni	IMIDZB	$Zn_2(Im)_4$	H_2O	nonporous[c]	2
coi	EQOCOC	$Zn_4(Im)_8$	H_2O	nonporous[c]	3
moc	KUMXEW	$Zn_4(Im)_8(HIm)$	ionic liquid	nonporous[c]	4
SOD	SALEM-2	$Zn(Im)_{1.7}(mIm)_{0.3}$	SALE[b]	6	5
cag	ZIF-4	$Zn_2(Im)_4$	DMF	6	6
cag	VEJYUF01	$Zn_2(Im)_4$	DMF	6	7
BCT	ZIF-1	$Zn_2(Im)_4$	DMF	8	6
BCT	VEJYEP01	$Zn_2(Im)_4$	DMA	8	7
BCT	ZIF-2	$Zn_2(Im)_4$	DMF	8	6
BCT	VEJYIT01	$Zn_2(Im)_4$	DMF	8	7
BCT	ZIF-64	$Zn_4(Im)_8$	DMF	8	8
MER	ZIF-10	$Zn(Im)_2$	DMF	8	6
MER	mer-MeMeCH$_2$	$Zn_{16}(Im)_{32}$	MeMeCH$_2$	8	11
DFT	ZIF-3	$Zn(Im)_2$	DMF+NMP	8	6
DFT	HIFVOI	$Zn(Im)_2$	NMP	8	7
GIS	ZIF-6	$Zn(Im)_2$	DMF	8	6
GIS	HIFVUO	$Zn(Im)_2$	DEF	8	7
nog	HIFWAV	$Zn_5(Im)_{10}$	DEF	8	7
neb	-	$Zn(Im)_2$	pyridine	8	9
zec	HICGEG	$Zn_5(Im)_{10}$	DEF	10	7
-	-	$Zn_{10}(Im)_{20}$	DBF	10	10
CAN	**CAN-[Zn(Im)$_2$]**	**Zn$_3$(Im)$_6$**	**DBF**	**12**	**Our**
AFI	**AFI-[Zn(Im)$_2$]**	**Zn(Im)$_2$**	**DPF**	**12**	**Our**

a: ionic liquid=1-ethyl-3-methylimidazolium bis[(trifluoromethyl) sulfonyl]imide; DMF=dimethylformamide; DMA=dimethylacetamide; DEF=diethylformamide; NMP=N-methylpyrrolidone; DBF= dibutylformamide; DPF=dipropylformamide;MeMeCH2=1,7,11,15,21,23,25,28-octamethyl-2,20:3,19-dimetheno-1H,21H,23H,25Hbis[1,3]dioxocino[5,4-i:5',4'-i']benzo[1,2-d:5,4-d']-bis[1,3]benzodioxocin.

b: SALE: obtained by solvent-assisted linker exchange.

c: nonporous (primarily 4-membered ring).

(1) Phan, A.; Doonan, C. J.; Uribe-Romo, F. J.; Knobler, C. B.; O'Keeffe, M.; Yaghi, O. M. *Acc. Chem. Res.* **2010**, *43*, 58–67.

(2) Lehnert, R.; Seel, F. Z. *Anorg. Allg. Chem.***1980**, *464*, 187–194.

(3) Tian, Y. Q.; Cai, C. X.; Ren, X. M.; Duan, C. Y.; Xu, Y.; Gao, S.; You, X. Z. *Chem. Eur. J.* **2003**, *9*, 5673–5685.

(4) Martins, G. A. V.; Byrne, P. J.; Allan, P.; Teat, S. J.; Slawin, A. M. Z.; Li, Y.; Morris, R. E. *Dalton Trans.* **2010**, *39*, 1758–1762.
(5) Karagiaridi, O.; Lalonde, M. B.; Bury, W.; Sarjeant, A. A.; Farha, O. K.; Hupp, J. T. *J. Am. Chem. Soc.* **2012**, *134*, 18790−18796
(6) Park, K. S.; Ni, Z.; Côté, A. P.; Choi, J. Y.; Huang, R. D.; Uribe-Romo, F. J.; Chae, H. K.; O'Keeffe, M.; Yaghi, O. M. *Proc. Natl. Acad. Sci. USA* **2006**, *103*, 10186–10191.
(7) Tian, Y. Q.; Zhao, Y. M.; Chen, Z. X.; Zhang, G. N.; Weng, L. H.; Zhao, D. Y. *Chem. Eur. J.* **2007**, *13*, 4146–4154.
(8) Banerjee, R.; Phan, A.; Wang, B.; Knobler, C.; Furukawa, H.; O'Keeffe, M.; Yaghi, O. M. *Science* **2008**, *319*, 939–943.
(9) Schroder, C. A.; Baburin, I. A.; Wullen, L. v.; Wiebcke, M.; Leoni, S. *CrystEngComm* **2013**, *15*, 4036–4040.
(10) Shi, Q.; Kang, X. Z; Shi, F. N.; Dong, J. X. *Chem. Commun.* **2015**, *51*, 1131–1134.
(11) Ramirez, J. R.; Yang, H. Y.; Kane, C. M.; Ley, A. N.; Holman, K. T. *J. Am. Chem. Soc.* **2016**, *138*, 12017–12020.

Table S3. Lists of representative ZIFs and their textural properties.

RCSR topoIogy or zeolite code	Type material	Framework formula[a]	Surface area (Langmuir) $m^2 g^{-1}$	Surface area (BET) $m^2 g^{-1}$	Pore volume $cm^3 g$	Ref.
SOD	ZIF-8	$Zn(mIm)_2$	1810	1630	0.64	1
SOD	ZIF-90	$Zn(ICA)_2$	1320	1270	0.58	2
RHO	ZIF-93	$Zn(4me5alIm)_2$	-	864	-	3
RHO	ZIF-71	$Zn(dclIm)_2$	-	652	-	3
CAN	**CAN-$[Zn(Im)_2]$**	**$Zn_3(Im)_6$**	**1401**	**1178**	**0.54**	**Our**
AFI	**AFI-$[Zn(Im)_2]$**	**$Zn(Im)_2$**	**1628**	**1386**	**0.64**	**Our**

a: mIm=2-methylimidazolate; Ica=imidazolate-2-carboxyaldehyde; 4me5alIm=4-methylimidazole-5-carbaldehyde; clbIm=4,5-dichloroimidazolate.

(1) Park, K. S.; Ni, Z.; Côté, A. P.; Choi, J. Y.; Huang, R. D.; Uribe-Romo, F. J.; Chae, H. K.; O'Keeffe, M.; Yaghi, O. M. *Proc. Natl. Acad. Sci. USA* **2006**, *103*, 10186–10191
(2) Morris, W.; Doonan, C. J.; Furukawa, H.; Banerjee, R.; and Yaghi O. M. *J. Am. Chem. Soc.* **2008**, *130*, 12626–12627.
(3) Morris, W.; Leung, B.; Furukawa, H.; Yaghi, O. K.; He, N.; Hayashi, H.; Houndonougbo Y.,; Asta, M.; Laird, B. B.; Yaghi O. M. *J. Am. Chem. Soc.* **2010**, *132*, 11006–11008.

Table S4. Crystallographic data and structure refinement summary for CAN-[$Zn(Im)_2$].

Compound	CAN-[$Zn(Im)_2$]
Empirical Formula	$C_{63}\ H_{93}\ N_{27}\ O_3\ Zn_6$
Formula weight	1668.86
Temperature	293(2) K
Wavelength	1.54184 Å
Crystal system, Space group	Orthorhombic, *Pnma*
Unit cell dimensions	*a*= 9.6256 (8) Å alpha = 90 deg. *b*= 23.436(2) Å beta = 90 deg. *c*= 41.593(3) Å gamma = 90 deg.
Volume	9382.8(13) $Å^3$
Z, Calculated density	4, 1.181 g/cm^3
Absorption coefficient	2.091 mm^{-1}
F(000)	3456
Crystal size	0.27 x 0.10 x 0.07 mm
Theta range for data collection	3.70 to 66.05 deg.
Limiting indices	-11<=h<=6, -26<=k<=27, -49<=l<=46
Reflections collected / unique	19363 / 8300 [$R_{(int)}$ = 0.1207]
Completeness to theta = 66.05	98.7 %
Absorption correction	Semi-empirical from equivalents
Max. and min. transmission	0.8674 and 0.6021
Refinement method	Full-matrix least-squares on F^2
Data / restraints / parameters	8300 / 5 / 471
Goodness-of-fit on F^2	1.058
Final *R* indices [I > 2sigma (I)]	R_1 = 0.1144, wR_2 = 0.2568
R indices (all data)	R_1 = 0.2397, wR_2 = 0.3168
Largest diff. peak and hole	1.419 and -0.594 $e^-\ A^{-3}$

Table S5. Crystallographic data and structure refinement summary for CAN-[$Zn(Im)_2$] (without the guest molecules).

Compound	CAN-[$Zn(Im)_2$]
Empirical Formula	$C_{36}\ H_{36}\ N_{24}\ Zn_6$
Formula weight	1197.11
Temperature	293(2) K
Wavelength	1.54184 Å
Crystal system, Space group	Orthorhombic, *Pnma*
Unit cell dimensions	*a*= 9.6256 (8) Å alpha = 90 deg. *b*= 23.436(2) Å beta = 90 deg. *c* = 41.593(3) Å gamma = 90 deg.
Volume	9382.8(13) $Å^3$
Z, Calculated density	4, 0.847 g/cm^3
Absorption coefficient	1.925 mm^{-1}
F(000)	2400
Crystal size	0.27 x 0.10 x 0.07 mm
Theta range for data collection	3.70 to 66.05 deg.
Limiting indices	-11<=h<=6, -26<=k<=27, -49<=l<=46
Reflections collected / unique	19592 / 8386 [$R_{(int)}$ = 0.0997]
Completeness to theta = 66.05	99.7 %
Absorption correction	Semi-empirical from equivalents
Max. and min. transmission	0.8770 and 0.6245
Refinement method	Full-matrix least-squares on F^2
Data / restraints / parameters	8386 / 0 / 301
Goodness-of-fit on F^2	1.047
Final *R* indices [I > 2sigma (I)]	R_1 = 0.0833, wR_2 = 0.1608
R indices (all data)	R_1 = 0.1635, wR_2 = 0.1756
Largest diff. peak and hole	1.445 and -0.354 $e^- A^{-3}$

Table S6. The results of the Rietveld analysis of for AFI-[$Zn(Im)_2$] (without the guest molecules).

Compound	AFI-[$Zn(Im)_2$]
Empirical Formula	$C_6H_6N_4Zn$
Temperature (K)	298(3)
Crystal system	hexagonal
Space group	*P*6/*mcc*
a/Å	26.437
c/Å	16.632
V/Å^3	10066.9
Z	24
R_p [a]	5.73%
R_{wp} [b]	9.18%

[a] $R_p = \Sigma|cY^{sim}(2\theta_i) - I^{exp}(2\theta_i) + Y^{back}(2\theta_i)|/\Sigma|I^{exp}(2\theta_i)|$.

[b] $R_{wp} = \{w_p[cY^{sim}(2\theta_i) - I^{exp}(2\theta_i) + Y^{back}(2\theta_i)]^2/\Sigma w_p[I^{exp}(2\theta_i)]^2\}^{1/2}$, and $w_p = 1/I^{exp}(2\theta_i)$.